How to cite: *Angew. Chem. Int. Ed.* **2025**, *64*, e202421302
doi.org/10.1002/anie.202421302

Oxaboroles Hot Paper

Rhodium-mediated Assembly of New Heterocycles: From Borylenes to Oxaboroles

*Shou-Jen Hsiang and Paul G. Hayes**

Abstract: Base-stabilized rhodium borylene complex κ^2-*L*(CO)Rh(BMes), **2**; κ^2-*L* = κ^2-NN'-Rh,κ^1-N–B-(2,5-[^{i}Pr$_2$P=N(4-^{i}PrC$_6$H$_4$)]$_2$-N'(C$_4$H$_2$)$^-$); Mes = mesityl, reacts with a series of alkynes (PhC≡C–R; R = Ph, Me, CO$_2$Et, H) to yield unique structures whereby the alkyne has regioselectively added across boron and the carbon atom of a CO ligand. The resulting complexes, *L*Rh[C(O)C(Ph)C(R)B(Mes)], **3^R**, react with additional CO to afford cycle-containing products, *L*(CO)Rh(PhCCR = *B*MesOC), **5^R**, that ultimately release highly functionalized organic heterocycles of the form PhC = *C*RBMesOC = NPipp (Pipp = 4-^{i}PrC$_6$H$_4$), **6**. These oxaboroles, which were assembled from a primary hydroborane, CO, an alkyne, and an azide-generated NPipp, are structurally analogous to two of the five boron-containing therapeutics approved by the FDA.

Introduction

Transition metal (TM) assisted assembly of value-added products from simple molecular building blocks is essential for meeting the demand of the high throughput chemical industry, and the ever-increasing growth of green chemistry initiatives which aim for high levels of atom economy. The ubiquity of carbonyl (C=O) functional groups in pharmaceutically-relevant molecules, which play key roles in orienting active sites and participating in intermolecular interactions, is well documented.[1] Carbon monoxide, the most simple multiply bonded carbon–oxygen moiety, is therefore an appealing C1 substrate for the efficient synthesis of carbonyl-containing compounds. Given that the CO ligand is one of the most common donors in coordination chemistry, TM complexes that can activate, and subsequently install, CO into complicated architectures are attractive.[2] Accordingly, the scientific literature is replete with examples of TM-assisted activation of carbon monoxide in processes akin to industrially important Fischer–Tropsch, Pauson–Khand and hydroformylation reactions.[3] Even so, the preparation of structurally complex "fine chemicals" *via* the selective combination of CO and multiple other small molecules remains synthetically challenging.[3a] A notable recent achievement is the catalytic carbonylation of alkynes to form retinoid esters, using a one-pot methodology that employs acetylenes, alcohols, and carbon monoxide (Scheme 1a).[3a,4] Kawatsura reported another elegant example wherein the [2+2+1] cycloaddition of carbon monoxide and disubstituted internal alkynes afforded highly functionalized heterocycles (Scheme 1b).[3a,5] More recently, Kobayashi presented Suzuki–Miyaura cross-coupling reactions in the presence of CO gas to yield diaryl ketones (Scheme 1c).[3a,6]

Boron-containing molecules are perhaps best known for their use in Suzuki–Miyaura cross-coupling processes, wherein the boron atom is discarded during the C–C bond forming reaction.[7] In recent decades, however, the development of technologies that capitalize upon the unique properties of boron has increased dramatically. Transition metal free catalysis, for example, often leverages the Lewis acidic properties of boron for bond activation purposes, *in lieu* of formal redox processes prevalent in traditional metal-mediated pathways.[8] On the pharmaceutical side, since the anti-cancer capabilities of bortezomib were discovered in 2003, four additional boron-containing drugs, all of which feature a boron heterocycle, have received FDA-approval.[9]

Previously, we disclosed that a rhodium carbonyl complex supported by a κ^3-*NNN* pincer ligand, *L*RhCO (**1**; *L* = κ^3-*NNN*' = 2,5-[^{i}Pr$_2$P=N(4-^{i}PrC$_6$H$_4$)]$_2$-N'(C$_4$H$_2$)$^-$), is able to dehydrogenate group 13 and 14 molecules.[10] In particular, the reaction between **1** and H$_2$BMes (Mes = mesityl), releases H$_2$ gas and generates the base-stabilized rhodium

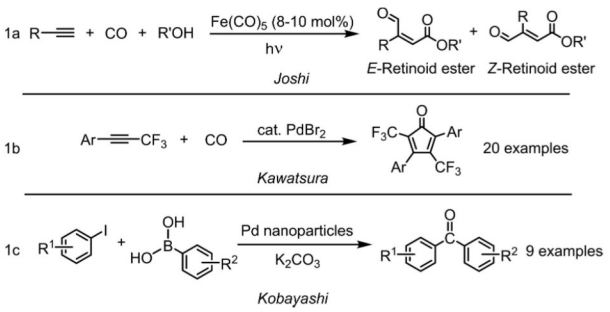

Scheme 1. Recent examples of direct CO incorporation into highly functionalized molecules.

[*] S.-J. Hsiang, Prof. Dr. P. G. Hayes
Department of Chemistry and Biochemistry
University of Lethbridge
4401 University Dr. W., Lethbridge, AB (Canada)
E-mail: p.hayes@uleth.ca

borylene complex κ^2-*L*(CO)Rh(BMes) (**2**; κ^2-*L* = κ^2-NN'-Rh,κ^1-N–B).[10c] The activation of primary boranes, and subsequent use of the resultant species as :BR synthons, is an appealing alternative to hydroboration for the synthesis of structurally complex boranes. Such compounds may then be used further downstream as high value substrates in cross-coupling reactions, as standalone reagents, or as pharmaceutical precursors. For example, borylene transfer to alkynes generally produces three membered borirene heterocycles, as demonstrated by Braunschweig et al. with their [$(OC)_5M{=}B{=}N(SiMe_3)_2$] (M = Cr, Mo) complexes (Scheme 2a).[11] The same group also reported stepwise borylene metathesis that proceeds through an isolable [2+2] cycloaddition intermediate that contains a Mn–B-(^{t}Bu)–O–C(Ph)$_2$ heterocycle, exhibiting the non-innocence of the benzophenone carbonyl group (Scheme 2b).[12]

As our rhodium borylene compounds are Lewis-base stabilized, we sought to investigate their reactivity with alkynes, in contrast to work previously published on terminal borylenes and aminoborylenes. Remarkably, reaction of complex **2** with diphenylacetylene did not undergo elimination of the anticipated borirene product, but instead generated an isolable species that features formal alkyne addition across boron and the carbon atom of the CO ligand (Scheme 3). Herein we detail our studies into the generality of this chemistry, as well as the subsequent release of novel five-membered oxaborole species, uniquely assembled from CO, BMes, NPipp (Pipp = 4-^{i}PrC$_6$H$_4$), and PhC≡CR. To the best of our knowledge, this class of molecule, which boasts a remarkable degree of built-in functionality sourced from simple substrates, is unprecedented.

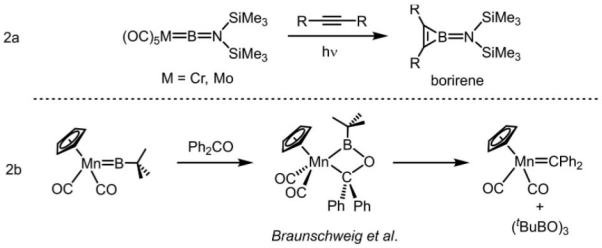

Scheme 2. a) Transfer of a terminal aminoborylene to alkynes; b) Borylene metathesis with benzophenone.

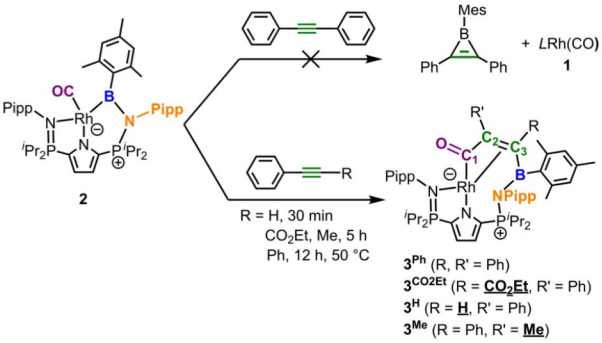

Scheme 3. Reaction of complex **2** with a series of alkynes (Ph–C≡C–R, R = Ph, Me, CO_2Et, H) to yield complexes **3**.

Results and Discussion

Reaction of Complex 2 with Alkynes

Starting from κ^2-*L*Rh(BMes), complex **2**, reaction with diphenylacetylene was attempted in an effort to establish if formal borylene transfer is possible. Surprisingly, the ^{31}P NMR spectrum, recorded after heating at 50 °C for 2 hours in benzene-d_6, revealed two new resonances in a 1:1 ratio (δ 51.8 and 44.7), as opposed to the anticipated regeneration of monocarbonyl **1** (δ 58.4) and concomitant release of 1-mesityl-2,3-diphenyl-1*H*-borirene (Scheme 3). Close examination of the corresponding ^{1}H and ^{13}C NMR spectra indicated two sets of aromatic and aliphatic resonances for the acetylene moiety, suggesting an unsymmetric product. Additionally, free rotation about the B–$C_{mesityl}$ bond is restricted on the NMR timescale, resulting in three distinct CH_3 resonances in the ^{1}H NMR spectrum. These spectroscopic signatures contradicted the formation of a simple alkyne coordination product, prompting further investigation into the identity of the complex. Gratifyingly, an X-ray crystal structure obtained from a moderately diffracting single crystal elucidated the compound's connectivity, wherein the alkyne has formally added across the Rh carbonyl and borylene functionalities, affording κ^2-*L*Rh[C-(O)C(Ph)C(Ph)B(Mes)], **3^{Ph}** (Figure 1, top left, *vide infra*).

When considering the structure of **3^{Ph}**, the newly formed C1(O)–C2(Ph)–C3(Ph)–B(Mes) framework, and its interaction with rhodium, is worthy of discussion. The ^{13}C NMR resonances for C2 and C3, at δ 140.0 and 84.0, respectively (assigned in relation to other complexes in the series, see below), indicate prominent polarization in the C2–C3 bond compared to δ 90.2 in symmetrical diphenylacetylene. The upfield shift in the C3 resonance, despite the proximity of C3 to the Lewis acidic boron atom, suggests a decrease in the C2–C3 bond order. Meanwhile, the downfield shifted C2 resonance is consistent with its proximity to the newly formed carbonyl functionality (C1 = O). A downfield shift was also observed for the ^{31}P NMR resonance assigned to the phosphorus atom in the phosphinimine bound to boron (δ 44.7, *c.f.* δ 37.8 in complex **2**), suggesting increased polarization in the $^{\delta+}$P–$^{\delta-}$N bond, which is well documented to possess substantial ylidic character.[10a,13] Unfortunately, the low quality of the X-ray crystal data for complex **3^{Ph}** prevents a detailed discussion of the metrical parameters; nonetheless, it is clear that C1, C2, and C3 each exhibit trigonal planar geometry that is consistent with formal sp^2 hybridization (Figure 1, top left). Notably, C2 and C3 are approximately equidistant from rhodium, implying η^2-coordination of the alkene. Geometry at boron is only slightly distorted from trigonal planar (Σ_{angles} = 353.6°), arguing against substantial Rh–B bonding. At 1734 cm^{-1} the ν_{CO} stretching frequency is higher than related neutral rhodium acyl species, but is comparable to anionic

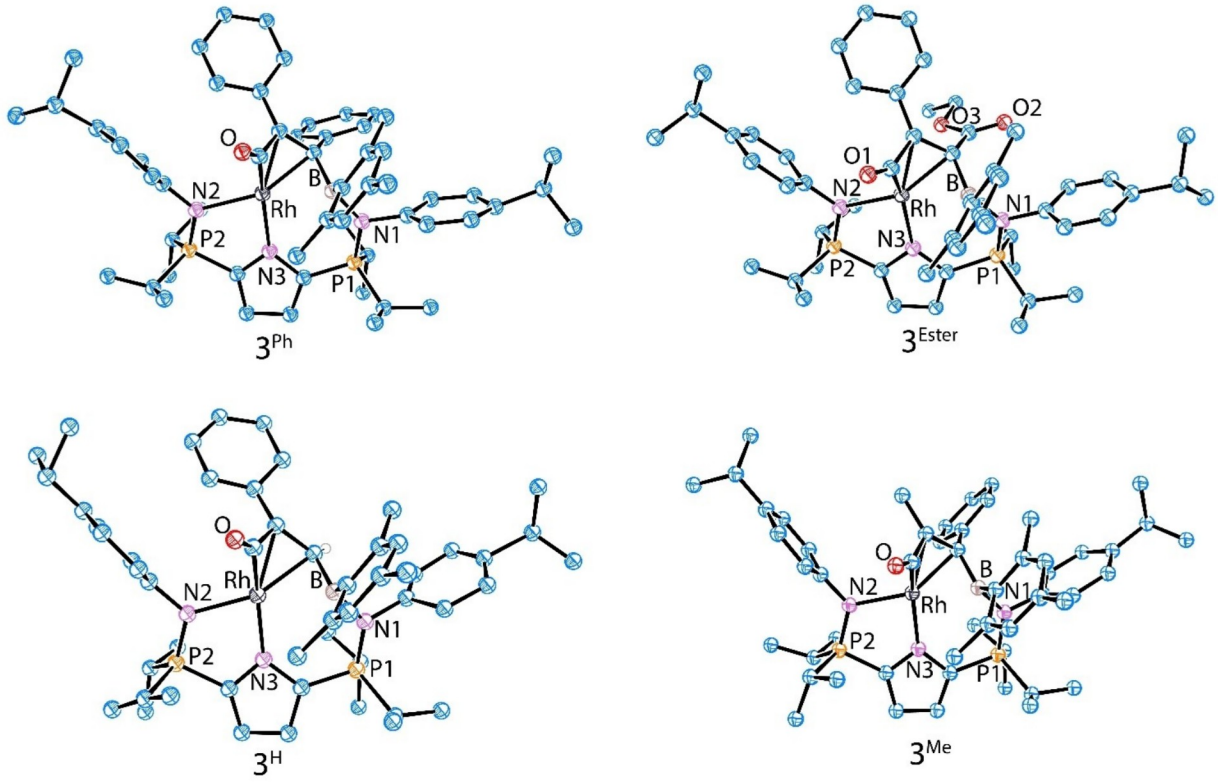

Figure 1. Connectivity structures of $\mathbf{3^{Ph}}$, $\mathbf{3^{CO2Et}}$, $\mathbf{3^{H}}$, and $\mathbf{3^{Me}}$ depicted with no thermal ellipsoid probabilities shown. Hydrogen atoms, apart from the C3-bound H in $\mathbf{3^{H}}$, disorder models, and co-crystallized solvent moieties have been removed for clarity.

$[AsPh_4]_2[(EtCO)Rh(CO)I_3]_2$ (1768 cm^{-1}).[14] Anionic rhenium acyl complexes have also been documented to exhibit higher ν_{CO} wavelengths than their neutral counterparts.[15] Given this information, we consider the most appropriate canonical structure to bear formal charges on rhodium and phosphorus, which maintains a metal oxidation state of +1 and an electron count of 16 at the metal center.

In order to garner a better understanding of the reaction between **2** and diphenylacetylene (PhC≡CPh), as well as the unusual bonding within the product, three additional alkynes, each with different steric and/or electronic properties, were selected to probe the generality of this chemistry. Reaction of complex **2** with an excess of ethyl-3-phenylpropiolate (PhC≡CO_2Et) in toluene, either at ambient temperature for five hours, or at 50 °C for one hour, led to isolation of κ^2-*L*Rh[C(O)C(Ph)C(<u>CO_2Et</u>)B(Mes)], $\mathbf{3^{CO2Et}}$. Reaction of complex **2** with excess phenyl acetylene (PhC≡CH), for 30 minutes at ambient temperature afforded κ^2-*L*Rh[C(O)C(Ph)C(<u>H</u>)B(Mes)], $\mathbf{3^{H}}$, whereas 1-phenyl-1-propyne (PhC≡CMe), required more judicious conditions to give the addition product κ^2-*L*Rh[C(O)C(<u>Me</u>)C(Ph)B-B(Mes)], $\mathbf{3^{Me}}$, in 42 % yield (Scheme 3). While slow conversion to $\mathbf{3^{Me}}$ was observed when the reaction was conducted over five hours at ambient temperature, prolonged heating led to darkening of the solution and the appearance of multiple new unidentified resonances in the ^{31}P and ^{1}H NMR spectra.

Remarkably, multinuclear NMR spectroscopy and X-ray crystallography confirmed that reactions with ethyl-3-phenylpropiolate and phenyl acetylene proceeded regio-specifically, wherein the phenyl substituent is adjacent (C2) to the carbonyl group (as opposed to boron) in the products (Figure 1, top right, bottom left). Conversely, reaction between **2** and 1-phenyl-1-propyne is predominantly (>85 % by NMR spectroscopy) regioselective for the other isomer, placing the phenyl group at C3 (Figure 1, bottom right). Careful examination of the ^{31}P NMR spectrum of $\mathbf{3^{Me}}$ revealed prominent resonances at δ 51.7 and 42.9 in a 1:1 ratio, as well as a lower intensity set at δ 50.7 and 43.2, postulated to be the minor regioisomer.

In all three unsymmetric alkyne addition products, $\mathbf{3^{H}}$, $\mathbf{3^{CO2Et}}$ and $\mathbf{3^{Me}}$, free rotation about the B–$C_{mesityl}$ bond is once again restricted on the ^{1}H NMR timescale. 2-Dimensional ^{1}H-^{13}C HMBC and HSQC NMR experiments confirmed that the C2 and C3 resonances in $\mathbf{3^{H}}$ and $\mathbf{3^{CO2Et}}$ are downfield and upfield shifted, respectively, compared to free alkyne. Meanwhile, the different regioselectivity in $\mathbf{3^{Me}}$ led to both C2 and C3 being downfield shifted compared to 1-phenyl-1-propyne (δ 144.1 and 93.1, *c.f.* δ 86.2 and 80.5 in PhC≡CMe). Given that there is a preference for electron donating groups adjacent to the rhodium carbonyl (Me > Ph > H ≫ CO_2Et), it is likely that there is positive charge buildup on C2 in the transition state, though it is unclear if the reaction proceeds in a concerted or stepwise fashion (Scheme 3, *vide supra*).

Unfortunately, this class of compound crystallizes in low diffracting clusters, and despite exhaustive efforts, we were unable to obtain high quality, solid-state data suitable for metrical discussions (See Supporting Information Table S2).

Reaction of Complexes 3 with CO

With a series of alkyne insertion products in hand, it was postulated that addition of CO gas might release a functionally rich organic molecule, along with concomitant generation of monocarbonyl **1**. To this end, complex $\mathbf{3}^{\mathbf{CO2Et}}$, which possesses a diagnostic C3-bound ester group, was selected for probing experiments. One atmosphere of CO gas was added to a *J*-Young NMR tube charged with a degassed benzene-d_6 solution of $\mathbf{3}^{\mathbf{CO2Et}}$. Progress of reaction was monitored via ^{31}P NMR spectroscopy and within two hours at ambient temperature signals for $\mathbf{3}^{\mathbf{CO2Et}}$ were completely supplanted by two equal intensity resonances at δ 58.3 and −0.8. Upon careful scrutiny it was established that conversion to this unidentified species proceeded through a transient intermediate ($\mathbf{5}^{\mathbf{CO2Et}}$, see below) which gives rise to peaks at δ 56.4 and 46.7. Notably, the chemical shift of the signal at δ −0.8 is too far upfield for a phosphinimine bound to a metal center, but is consistent with either a free phosphinimine or reduced P(III) nucleus.[10a,16] An X-ray diffraction study of single crystals corroborated the NMR spectroscopic evidence. Specifically, the NPipp group was excised by P–N bond cleavage, yielding the dicarbonyl rhodium complex $L^2Rh(CO)_2$ ($L^2 = \kappa^2$-[2-^{i}Pr$_2$P=N-(4-^{i}PrC$_6$H$_4$)-5-P^{i}Pr$_2$]-N'(C$_4$H$_2$)$^-$), **4**, (Figure 2) as the sole metal-containing product. Inspection of the ^{1}H NMR spectrum revealed a new set of resonances attributed to the phenyl and ester moieties of the former alkyne, the liberated NPipp, and the boron-bound mesityl group. The substantially different chemical shifts indicate distinct chemical environments from complex $\mathbf{3}^{\mathbf{CO2Et}}$, and coupled with their matching relative integrations, suggest formation of a single new organic compound.

Exposure of $\mathbf{3}^{\mathbf{Ph}}$ to CO for 14 hours at 45 °C in benzene solvent also afforded complex **4**, though in this case no evidence for intermediates was observed by either ^{31}P or ^{13}C NMR spectroscopy. Conversely, reaction of $\mathbf{3}^{\mathbf{H}}$, which lacks a C1 substituent, with 1 atm of CO, permitted isolation of κ^2-*L*(CO)Rh(PhCCH = *B*MesOC), $\mathbf{5}^{\mathbf{H}}$, (^{31}P: δ 54.7 and 45.1). Complex $\mathbf{5}^{\mathbf{H}}$ forms rapidly (<10 minutes) at ambient temperature. Removal of residual CO prevents conversion to complex **4**, thereby allowing for complete characterization by NMR spectroscopy (Scheme 4, top). Free rotation about the B–C$_{mesityl}$ bond, as indicated by a single resonance for the *ortho*-CH$_3$ groups, implies less steric hindrance at boron in $\mathbf{5}^{\mathbf{H}}$, compared to $\mathbf{3}^{\mathbf{H}}$. A 2D-HSQC experiment allowed a broad singlet in the ^{13}C NMR spectrum (δ 119.0) to be attributed to C3, which is downfield shifted from δ 70.3 in $\mathbf{3}^{\mathbf{H}}$. The substantial change in chemical shift is expected because of electron delocalization throughout the ring, as well as proximity to the adjacent Lewis acidic boron atom. Likewise, the ^{1}H NMR signal for the C3-bound hydrogen moved from δ 4.85 in $\mathbf{3}^{\mathbf{H}}$ to δ 6.15 in $\mathbf{5}^{\mathbf{H}}$. Carbon 2, which exhibits weak coupling to ^{103}Rh ($^1J_{C-Rh}$ = 12 Hz), was established by 2D-HMBC experiments to resonate at δ 175.1. Finally, C1, which originated from the activated CO ligand, appears as a doublet of doublets centered at δ 105.7 ($^1J_{C-Rh}$ = 41 Hz, $^2J_{C-P}$ = 10 Hz). Coupling to phosphorus supports interaction between C1 and the phosphinimine nitrogen, as required for generation of the new C1–C2–C3–B–O ring (Scheme 4). A new ^{13}C resonance at δ 196.4, with a $^1J_{C-Rh}$ coupling constant of 83 Hz, is attributed to a newly coordinated CO ligand. Addition of an atmosphere of CO gas, under ambient conditions, to compound $\mathbf{5}^{\mathbf{H}}$ resulted in exclusive conversion to dicarbonyl **4**, along with release of the cyclic organic product PhC= CHBMesOC=NPipp, $\mathbf{6}^{\mathbf{H}}$. Given the identity of **4** (Figure 2) and $\mathbf{5}^{\mathbf{Me}}$, as confirmed by X-ray crystallography (*vide infra*, Figure 3), it is reasonable to assume that release of compounds **6** (from **5**) involves cleavage of the P–N bond closest to C1 (Scheme 4, bottom).

When excess CO was introduced to a benzene-d_6 solution of $\mathbf{3}^{\mathbf{Me}}$, two ^{31}P NMR resonances similar to those

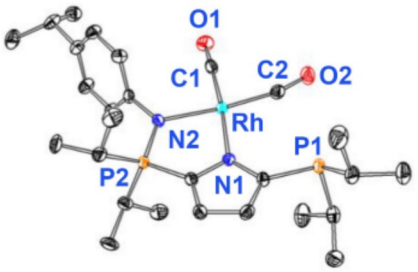

Figure 2. X-ray crystal structure of complex **4** with thermal ellipsoids represented at 50% probability. Hydrogen atoms removed for clarity. Selected bond lengths (Å) and angles [°]: C1–O1 1.130(5), C2–O2 1.134(5), Rh–N2 2.086(3), Rh–N1 2.079(3), N1–Rh–N2 84.1(1).

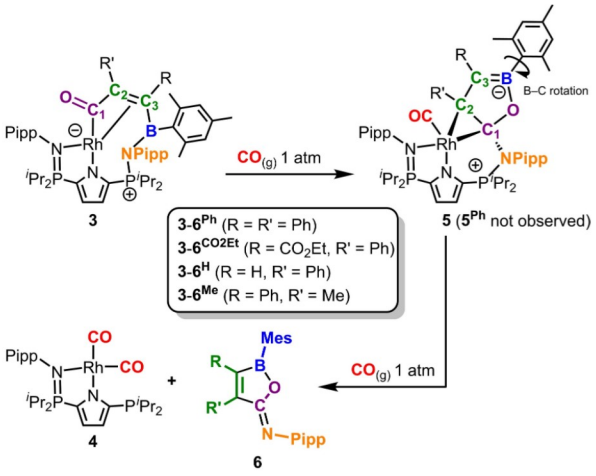

Scheme 4. Top: Reaction between complexes **3** and CO$_{(g)}$ to form cyclic intermediates $\mathbf{5}^{\mathbf{CO2Et}}$, $\mathbf{5}^{\mathbf{H}}$ and $\mathbf{5}^{\mathbf{Me}}$, respectively. $\mathbf{3}^{\mathbf{Ph}}$ is presumed to proceed through the analogous intermediate, but $\mathbf{5}^{\mathbf{Ph}}$ was not observed spectroscopically. Bottom: Reaction of complexes **5** with additional CO$_{(g)}$ to yield complexes **4** and cyclic oxaboroles **6**.

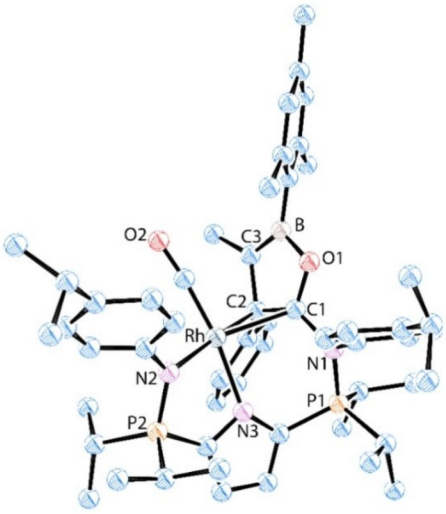

Figure 3. Connectivity structure of compound $\mathbf{5^{Me}}$ with no thermal ellipsoid probabilities shown. Hydrogen atoms, as well as disorder models removed for clarity.

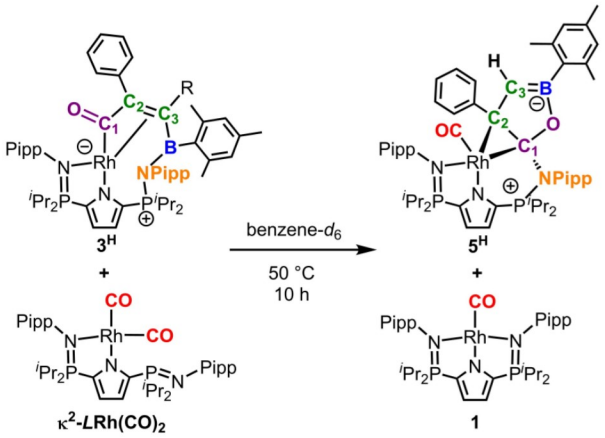

Scheme 5. Reaction of complex $\mathbf{3^H}$ with κ^2-*L*Rh(CO)$_2$ to afford $\mathbf{5^H}$ and monocarbonyl **1** via CO transfer from κ^2-*L*Rh(CO)$_2$.

observed for both $\mathbf{5^H}$ and $\mathbf{5^{CO2Et}}$, appeared at δ 54.4 and 45.1. These signals were quickly replaced by those corresponding to complex **4**. As previously mentioned, excessive heating during the preparation of $\mathbf{3^{Me}}$ darkened the solution and generated numerous unidentified signals in the ^{31}P NMR spectrum. Single crystals suitable for an X-ray diffraction study were grown from this reaction mixture and established to be $\mathbf{5^{Me}}$ (Figure 3). Although $\mathbf{5^{Me}}$ is presumably a minor by-product, likely arising from intermolecular CO transfer from one molecule of $\mathbf{3^{Me}}$ to another, its solid-state structure and spectroscopic signatures corroborate the proposed structures for $\mathbf{5^{Ph}}$, $\mathbf{5^H}$ and $\mathbf{5^{CO2Et}}$. While the low quality of the structure limits detailed discussion, notable metrics include C1–C2 and C2–C3 bond lengths of 1.52(2) Å and 1.55(2) Å, respectively, as well as a short B–C3 distance (1.35(2) Å), the combination of which led to the proposed canonical structure shown in Schemes 4 and 5. Boron maintains trigonal planar geometry ($\Sigma_{angles}=360°$), while C1 and C2 deviate slightly from planarity ($\Sigma_{angles}=355°$ and 347°, respectively).

In an effort to lend credence to the possibility of intermolecular CO transfer from one rhodium complex to another, κ^2-*L*Rh(CO)$_2$, a synthetic precursor to monocarbonyl **1**, was selected as a convenient stoichiometric source of CO, particularly on a milligram scale.[16] Heating a 1:1 mixture of $\mathbf{3^H}$ and κ^2-*L*Rh(CO)$_2$ in benzene-d_6 at 50 degrees for 10 hours led to complete consumption of both species, and exclusive formation of complexes **1** and $\mathbf{5^H}$ (Scheme 5).

High resolution mass spectrometric experiments using a direct injection orbitrap instrument unambiguously gave rise to peaks for the parent ions (M^+ or M+H) of each of the organic products $\mathbf{6^{Ph}}$, $\mathbf{6^{CO2Et}}$, $\mathbf{6^H}$, and $\mathbf{6^{Me}}$. Furthermore, spectra obtained from gas chromatography-mass spectrometry (GC-MS) experiments performed on a lower resolution instrument indicated fragmentation patterns consistent with that expected for compounds **6** (See Supporting Information Figures S21–S24). To the best of our knowledge, this highly functionalized heterocycle is unprecedented. The unsaturated C2–C3 bond, as well as the C1 bound imine, offer platforms for a wide range of future organic transformations. In addition, incorporation of an ester on C3 in $\mathbf{6^{CO2Et}}$, which is also ideal for subsequent derivation, is pharmaceutically relevant. Notably, benzoxaborole-containing tavaborole (Kerydin) and crisaborole (Eucrisa) represent two of the five boron-containing drugs that are currently FDA approved (Figure 4, left).[9a] Accordingly, related 3-substituted-2(5*H*)-oxaboroles and their derivatives have prompted numerous studies over the past five years that explore their utility as antimicrobial therapeutics and agrochemical solutions.[17]

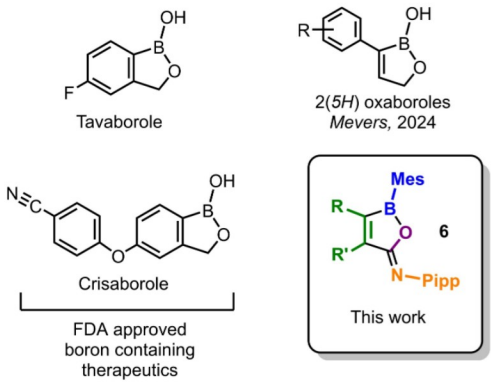

Figure 4. Structural comparison between FDA approved topical antifungal therapeutics tavaborole and crisaborole, 2(5*H*)oxaboroles studied by Mevers et al. as antimicrobial therapeutics,[17a] and oxaboroles **6**.

^{13}C NMR Labelling Studies

In order to unambiguously follow the carbonyl carbon (C1) throughout this unusual series of reactions, ^{13}C labelling studies were undertaken. ^{13}CO labelled borylene complex **[^{13}C]-2** was prepared, and as expected, exhibited a prominent doublet centered at δ 196.6 ($^{1}J_{C–Rh}$ = 88 Hz). The four alkyne addition products gave rise to downfield shifted C1 ^{13}C signals that ranged from δ 201.4 in **[^{13}C]-3^{CO2Et}** to δ 206.4 in **[^{13}C]-3^{Me}** (Table 1). The minor regioisomer of **[^{13}C]-3^{Me}** exhibited a low intensity labeled resonance at δ 203.3. When complexes **[^{13}C]-5** were synthesized *via* addition of natural abundance CO gas to complexes **[^{13}C]-3**, the labelled C1 resonances shifted dramatically upfield to δ 105.7–108.9 and appeared as doublets of doublets with distinct coupling to both rhodium ($^{1}J_{C–Rh}$ = 36–42 Hz) and the nearby phosphorus atom ($^{2}J_{C–P}$ = 10–11 Hz). The chemical shift can be rationalized by substantial electronic donation from the phosphinimine nitrogen, as well as a marked decrease in C–O multiple bond character. Finally, the isotopically enriched ^{13}C resonances in the extruded organic products (**[^{13}C]-6**) were observed between δ 157.4 and δ 176.9. Release from the organometallic complex to yield compounds **[^{13}C]-6** was corroborated by the fact that these signals exhibited no coupling whatsoever to either ^{31}P or ^{103}Rh. Furthermore, no signals consistent with isotopically enriched ^{13}C were observed bound to rhodium, indicating that the ^{13}C label in complexes **[^{13}C]-3** and **[^{13}C]-5** is not susceptible to exchange, nor is the reaction that yields **3** from **2** reversible under these conditions. This finding is additionally supported by the fact that no obvious decrease in labeled ^{13}C signal intensity was apparent even when the reaction mixture was exposed to a vast excess of natural isotopic abundant CO gas for a prolonged period. By contrast, the control reaction between isotopically enriched **[^{13}C]-2** and an atmosphere of unlabelled CO gas resulted in gradual decrease in signal intensity over an hour at ambient temperature. Finally, an excess of isotopically enriched ^{13}CO gas was added to **3^{H}**, ultimately affording diagnostic ^{13}C resonances for **4** at δ 186.2 (dd, $^{1}J_{C–Rh}$ = 69 Hz, $^{3}J_{C–P}$ = 10 Hz) and 183.2 (dd, $^{1}J_{C–Rh}$ = 70 Hz, $^{3}J_{C–P}$ = 10 Hz). No incorporation of ^{13}CO into oxaborole **6^{H}** was observed (See Supporting Information Figure 20).

When dicarbonyl **4** remains in the reaction mixture, gradual transition to a new product with ^{31}P NMR resonances at δ 54.3 and 38.9 was observed. Notably, the signal at δ 38.9 is a broad doublet with a large coupling constant ($^{1}J_{P–Rh}$ = 147 Hz), reminiscent of coupling exhibited by rhodium triphenylphosphine complexes. Diagnostic peaks pertaining to the unsymmetric L^2 ligand exist in the ^{1}H NMR spectrum, while the ^{13}C NMR spectrum displays no intense signals attributable to isotopically enriched ^{13}CO. This product is postulated to be dinuclear, resulting from coordination of the newly generated phosphine to rhodium in another molecule of **4**.

Computational Studies

The lack of high-quality X-ray data, as well as the novel bonding modes within this series of compounds, prompted us to explore computational methods to further our understanding. The idealized solution-phase geometries were calculated using density functional theory (DFT) at the def2SVP level of theory using Truhlar's SMD model (solvent = toluene).[18] All optimized structures matched closely with metrics obtained by X-ray diffraction analysis for the alkyne insertion products **3** (Rh–C1, Rh–C2, Rh–C3,

Table 1: Selected NMR resonances observed while monitoring the reaction between isotopically enriched **[^{13}C]-2** and various alkynes.

	^{31}P (P=N–Rh) (δ)	^{31}P (δ)	C1 ^{13}C ($^{1}J_{CRh}$, $^{2}J_{CP}$) (δ, Hz, Hz)
[^{13}C]-2 + diphenylacetylene			
[^{13}C]-3^{Ph}	51.8	44.7	203.7 (d, 22)
Intermediate		Not observed	
Organic Product (**6^{Ph}**)	–	–	176.9
[^{13}C]-2 + ethyl-3-phenylpropiolate			
[^{13}C]-3^{CO2Et}	51.6	45.6	201.4 (d, 22)
Intermediate (**[^{13}C]-5^{CO2Et}**)	56.4	46.7	108.9 (dd, 11, 36)
Organic Product (**[^{13}C]-6^{CO2Et}**)	–	–	157.4
[^{13}C]-2 + phenylacetylene			
[^{13}C]-3^{H}	48.2	45.1	206.1 (d, 21)
Intermediate (**[^{13}C]-5^{H}**)	54.7	45.1	105.7 (dd, 10, 41)
Organic Product (**[^{13}C]-6^{H}**)	–	–	157.9
[^{13}C]-2 + 1-phenyl-1-propyne			
[^{13}C]-3^{Me}	51.7	42.9	206.4 (d, 22)
Intermediate (**[^{13}C]-5^{Me}**)	54.4	45.1	108.0 (dd, 11, 42)
Organic Product (**[^{13}C]-6^{Me}**)	–	–	160.3

N–B, bond lengths all matched within 0.05, 0.02, 0.02 and 0.03 Å respectively). In all four optimized structures, C2 and C3 are equidistant from rhodium, and C1, C2, C3, and boron all exhibit trigonal planar geometry, supporting the previously described bonding motif (See Supporting Information Table S1, Figure 1). The calculated and experimental bond lengths for the borane-bound iminophosphorane P–N support single bond character; it is elongated compared to its rhodium coordinated counterpart. Examination of the localized natural bonding orbitals (NBOs) in these four complexes (with regard to the N–B interaction) revealed a formal σ-bonding NBO between the two atoms that is occupied by approximately two electrons (e.g. 1.939 in $\mathbf{3^{Ph}}$). Conversely, the C2–C3 π-bonding NBOs are only partial occupied (1.261–1.590), suggesting extensive electron delocalization and/or donation to the rhodium metal center. Second order perturbation analysis corroborated this interpretation, whereby a moderate ($E^{(2)}$: 41.82 kcal mol^{-1} in $\mathbf{3^{Ph}}$) donor-acceptor interaction was established between the C2–C3 π-bonding NBO and the vacant lp* orbital on rhodium. A stronger ($E^{(2)}$: 113.73 kcal mol^{-1} in $\mathbf{3^{Ph}}$) interaction was noted between the same C2–C3 π-bonding NBO and the Rh–C1 antibonding orbital. The p-orbital on boron appears to have little interaction with the C2–C3 π-system, and is instead involved in a strong ($E^{(2)}$: 29.13 kcal mol^{-1} in $\mathbf{3^{Ph}}$) donor-acceptor interaction with the lone pair on nitrogen N(lp)→B(p).

A hypothesized reaction intermediate between complexes **3** and **5**, wherein an equivalent of CO is coordinated to rhodium prior to cyclization, was modelled in an attempt to glean additional information about the reaction mechanism (Figure 5). Coordination of CO to the metal center appears to distort the geometry of the system so as to promote cyclization. Namely, in all four examples, the Rh–C1–C2–C3 torsion angle increases by approximately 10°, while C1–C2–C3–B decreases by a similar amount, bringing the carbonyl group closer in proximity to the boron atom. In all cases, the Rh–C2 and Rh–C3 distances elongate and the C2–C3 bond contracts (e.g. 2.251, 2.308, 1.407 Å *c.f.* 2.127, 2.144, 1.452 Å in $\mathbf{3^{Ph}}$). NBO analysis suggests an increase in orbital occupancy in the C2–C3 π-bonding NBOs. The natural charge distribution calculated for the boron atom (0.918) and C1 (0.615) revealed that they bear the highest localized positive charges in the system, aside from the phosphorus atoms, rendering them susceptible to nucleophilic attack.

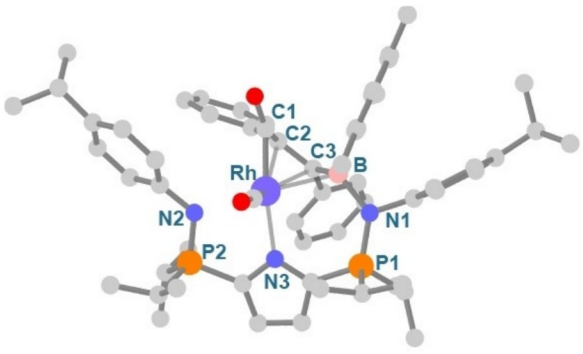

Figure 5. Optimized structure of a hypothesized reaction intermediate between complexes **3** and **5** wherein an equivalent of CO has coordinated to $\mathbf{3^{Ph}}$ prior to cyclization of the organic framework. Selected calculated bond lengths (Å): Rh–C1 1.947, Rh–C2 2.251, Rh–C3 2.308, C2–C3 1.407.

Conclusion

Overall, a remarkable series of sequential transformations between rhodium complex **1**, a primary borane, an alkyne, an auxiliary CO ligand, and the pincer ligand's phosphinimine NPipp group, yielded a new class of boron-containing compound, one with great potential utility for organic, organometallic, and pharmaceutical applications. The system is tolerant of a variety of alkynes, including terminal and ester substituted examples, and displays a high degree of regioselectivity when unsymmetric compounds are used. Isotopic labelling experiments unambiguously demonstrated that the carbonyl ligand in complex **2** is ultimately incorporated into the final oxaborole products.

Given the pharmaceutical relevance of the five-membered oxaborole structure, ongoing studies aim to further expand the substrate scope in this system and enhance our mechanistic understanding of the unique cyclization. Furthermore, we envision that sequential addition of $PippN_3$ and *L*Rh(COE) to complex **4** should spontaneously release N_2 and regenerate complex **1**, thereby completing the synthetic cycle.

Supporting Information

Supporting Information: Experimental details, NMR spectra, X-ray crystallographic data, and computational details. Deposition Number 2387421 (for **4**) contains the supplementary crystallographic data for this paper. These data are provided free of charge by the joint Cambridge Crystallographic Data Centre (CCDC) and Fachinformationszentrum Karlsruche Access Structures service. The authors have cited additional references within the Supporting Information.[19–25]

Acknowledgements

The authors acknowledge the Canada Foundation for Innovation and NSERC of Canada for a Discovery Grant to P.G.H. This research was enabled in part by resources provided by the Digital Research Alliance of Canada (alliancecan.ca). P.G.H. also thanks the University of Lethbridge for a Tier I Board of Governors Research Chair in Organometallic Chemistry.

Conflict of Interest

The authors declare no conflict of interest.

Data Availability Statement

The data that support the findings of this study are available in the supplementary material of this article.

Keywords: cyclization · alkyne · borylene · rhodium · oxaborole

[1] A. Renslo, in *The Organic Chemistry of Medicinal Agents* (Ed.: A. Renslo), McGraw-Hill Education, New York, NY, **2016**.

[2] B. F. Straub, *Angew. Chem., Int. Ed.* **2010**, *49*, 7622–7622.

[3] a) R. M. B. Carrilho, M. J. F. Calvete, G. Mikle, L. Kollár, M. M. Pereira, *Chin. J. Chem* . **2024**, *42*, 199–221; b) K. M. Brummond, J. L. Kent, *Tetrahedron* **2000**, *56*, 3263–3283.

[4] R. K. Joshi, N. Satrawala, *Tetrahedron Lett.* **2017**, *58*, 2931–2935.

[5] S. Murakami, T. Sonehara, K. Iwakami, H. Tsuji, M. Kawatsura, *Tetrahedron Lett.* **2019**, *60*, 598–601.

[6] T. Yasukawa, Z. Zhu, Y. Yamashita, S. Kobayashi, *Synlett* **2021**, *32*, 502–504.

[7] J. P. G. Rygus, C. M. Crudden, *J. Am. Chem. Soc.* **2017**, *139*, 18124–18137.

[8] a) S. Mummadi, C. Krempner, *Molecules* **2023**, *28*, 1340; b) L. Schweighauser, H. A. Wegner, *Chem. Eur. J.* **2016**, *22*, 14094–14103; c) V. Nori, F. Pesciaioli, A. Sinibaldi, G. Giorgianni, A. Carlone, *Catalysts* **2022**, *12*, 5.

[9] a) K. Messner, B. Vuong, G. K. Tranmer, *Pharmaceuticals* **2022**, *15*, 264; b) B. J. Wang, M. P. Groziak, in *Adv. Heterocycl. Chem., Vol. 118* (Eds.: E. F. V. Scriven, C. A. Ramsden), Academic Press, **2016**, pp. 47–90.

[10] a) S.-J. Hsiang, P. G. Hayes, *Chem. Eur. J.* **2024**, *30*, e202304302; b) C. S. MacNeil, P. G. Hayes, *Chem. Eur. J.* **2019**, *25*, 8203–8207; c) C. S. MacNeil, S.-J. Hsiang, P. G. Hayes, *Chem. Commun.* **2020**, *56*, 12323–12326.

[11] a) H. Braunschweig, T. Herbst, D. Rais, F. Seeler, *Angew. Chem. Int. Ed.* **2005**, *44*, 7461–7463; b) C. E. Anderson, H. Braunschweig, R. D. Dewhurst, *Organometallics* **2008**, *27*, 6381–6389.

[12] H. Braunschweig, M. Burzler, K. Radacki, F. Seeler, *Angew. Chem. Int. Ed.* **2007**, *46*, 8071–8073.

[13] a) K. Dehnicke, F. Weller, *Coord. Chem. Rev.* **1997**, *158*, 103–169; b) J. L. Lortie, M. Davies, P. D. Boyle, M. Karttunen, P. J. Ragogna, *Inorg. Chem.* **2024**, *63*, 6335–6345; c) I. M. Marin, A. Auffrant, *Eur. J. Inorg. Chem.* **2018**, *2018*, 1634–1644; d) W. W. Schoeller, T. Busch, E. Niecke, *Chem. Ber.* **1990**, *123*, 1653–1654.

[14] a) M. Bassetti, A. Capone, L. Mastrofrancesco, M. Salamone, *Organometallics* **2003**, *22*, 2535–2538; b) Y. Chen, D. Liu, Y. Yu, *RCS Adv.* **2017**, *7*, 49875–49882; c) J. Conradie, J. C. Swarts, *Organometallics* **2009**, *28*, 1018–1026; d) P. Das, M. Sharma, N. Kumari, D. Konwar, D. K. Dutta, *Appl. Organomet. Chem.* **2002**, *16*, 302–306; e) L. A. Howe, E. E. Bunel, *Polyhedron* **1995**, *14*, 167–173; f) B. D. Panthi, S. L. Gipson, A. Franken, *Inorg. Chim. Acta* **2015**, *425*, 176–181; g) S. I. Vdovenko, I. I. Gerus, V. P. Kukhar, *Spectrochim. Acta A.* **2008**, *71*, 779–785.

[15] A. C. Filippou, B. Lungwitz, G. Kociok-Ko"hn, I. Hinz, *J. Organomet. Chem.* **1996**, *524*, 133–146.

[16] C. S. MacNeil, K. E. Glynn, P. G. Hayes, *Organometallics* **2018**, *37*, 3248–3252.

[17] a) R. Campbell, N. W. Buchbinder, C. Szwetkowski, Y. Zhu, K. Piedl, M. Truong, J. B. Matson, W. L. Santos, E. Mevers, *ACS Med. Chem. Lett.* **2024**, *15*, 349–354; b) Z. He, D.-C. Huang, D. Guo, F. Deng, Q. Sha, M.-Z. Zhang, W.-H. Zhang, Y.-C. Gu, *Adv. Agrochem* **2023**, *2*, 185–195; c) K. Nowicki, J. Krajewska, T. M. Stępniewski, M. Wielechowska, P. Wińska, A. Kaczmarczyk, J. Korpowska, J. Selent, P. H. Marek-Urban, K. Durka, K. Woźniak, A. E. Laudy, S. Lulíński, *RSC Med. Chem.* **2024**, *15*, 1751–1772; d) A. L. Walker, A. Denis, R. P. Bingham, A. Bouillot, E. V. Edgar, A. Ferrie, D. S. Holmes, A. Laroze, J. Liddle, M.-H. Fouchet, A. Moquette, P. Nassau, A. C. Pearce, O. Polyakova, K. J. Smith, P. Thomas, J. H. Thorpe, L. Trottet, Y. Wang, A. Hovnanian, *Bioorg. Med. Chem. Lett.* **2019**, *29*, 126675.

[18] a) A. V. Marenich, C. J. Cramer, D. G. Truhlar, *J. Phys. Chem. B.* **2009**, *113*, 6378–6396; b) F. Weigend, *Phys. Chem. Chem. Phys.* **2006**, *8*, 1057–1065; c) F. Weigend, R. Ahlrichs, *Phys. Chem. Chem. Phys.* **2005**, *7*, 3297–3305.

[19] C. S. MacNeil, S.-J. Hsiang, P. G. Hayes, *Chem. Commun.* **2020**, *56*, 12323–12326.

[20] a) G. M. Sheldrick, *Acta Crystallogr., Sect. A: Found. Adv.* **2015**, *71*, 3–8; b) G. M. Sheldrick, *Acta Crystallogr., Sect. C: Struct. Chem.* **2015**, *71*, 3–8.

[21] Gaussian 16 C.01. M. J. Frisch, G. W. Trucks, H. B. Schlegel, G. E. Scuseria, M. A. Robb, J. R. Cheeseman, G. Scalmani, V. Barone, G. A. Petersson, H. Nakatsuji, X. Li, M. Caricato, A. V. Marenich, J. Bloino, B. G. Janesko, R. Gomperts, B. Mennucci, H. P. Hratchian, J. V. Ortiz, A. F. Izmaylov, J. L. Sonnenberg, Williams, F. Ding, F. Lipparini, F. Egidi, J. Goings, B. Peng, A. Petrone, T. Henderson, D. Ranasinghe, V. G. Zakrzewski, J. Gao, N. Rega, G. Zheng, W. Liang, M. Hada, M. Ehara, K. Toyota, R. Fukuda, J. Hasegawa, M. Ishida, T. Nakajima, Y. Honda, O. Kitao, H. Nakai, T. Vreven, K. Throssell, J. A. Montgomery Jr., J. E. Peralta, F. Ogliaro, M. J. Bearpark, J. J. Heyd, E. N. Brothers, K. N. Kudin, V. N. Staroverov, T. A. Keith, R. Kobayashi, J. Normand, K. Raghavachari, A. P. Rendell, J. C. Burant, S. S. Iyengar, J. Tomasi, M. Cossi, J. M. Millam, M. Klene, C. Adamo, R. Cammi, J. W. Ochterski, R. L. Martin, K. Morokuma, O. Farkas, J. B. Foresman, D. J. Fox, Wallingford, CT, **2016**.

[22] Y. Zhao, D. G. Truhlar, *Theor. Chem. Acc.* **2008**, *120*, 215–241.

[23] a) F. Weigend, *Phys. Chem. Chem. Phys.* **2006**, *8*, 1057–1065; b) F. Weigend, R. Ahlrichs, *Phys. Chem. Chem. Phys.* **2005**, *7*, 3297–3305.

[24] S. Grimme, J. Antony, S. Ehrlich, H. Krieg, *J. Chem. Phys.* **2010**, *132*.

[25] A. V. Marenich, C. J. Cramer, D. G. Truhlar, *J. Phys. Chem. B* **2009**, *113*, 6378–6396.

Manuscript received: November 2, 2024
Accepted manuscript online: January 14, 2025
Version of record online: January 21, 2025